Analysis of the High Bit-rate 1.55 μm Lightwave System with the Limited P-i-N Photodiode Bandwidth

M. Cvetković, P. Matavulj, J. Radunović and A. Marinčić

Abstract— **We analyze the impact of the limited P-i-N photodiode bandwidth on the performance of the 1.55 μm IM/DD (Intensity Modulation/Direct Detection) 10 Gb/s digital optical communication systems. The complete model of the optical communication system with the special accent on P-i-N photodiode is described. The computer simulation based on the developed model shows that the limited P-i-N photodetector bandwidth reduces the overshoot of the filtered signal at receiver. The proper selection of the P-i-N photodiode non-material parameters may improve the quality of signal detection at receiver side.**

I. Introduction

Optical communication IM/DD (Intensity Modulation/Direct Detection) systems represent one of the most spread configuration of the lightwave systems nowadays due to relatively simple structure and realization. Various detailed studies of the IM/DD digital optical system performance can be found in the literature [1], [2], [3]. However, these analysis assume that the photodetector at the receiving side of the system is ideal square-law device or that the photodetector bandwidth is much larger than the receiver filter bandwidth. In our paper we consider the case when the P-i-N photodetector bandwidth cannot be ignored in the analysis of the 1.55 μm optical system. Developed model described in section II includes all the relevant components of the typical IM/DD digital optical communication system. The results from the computer simulation of the optical system are presented in section III, while the summary and conclusion concerning the taken analysis are given in section IV.

II. Mathematical model

The analyzed lightwave system consists of optical transmitter, optical fiber and receiver. Single-mode MQW laser diode is considered as a optical transmitter. The signal is propagated through the single-mode optical fiber. Optical receiver consists of the P-i-N photodiode and the electric filter placed before sampling/detector unit.

While the laser diode is modeled with standard rate-equations, single-mode optical fiber, P-i-N photodiode and electrical filter are modeled with appropriate pulse responses of these devices. The output signal from each of these devices is obtained by calculating the convolutions of the input device signal and the appropriate device pulse response. This approach assumes that optical fiber, P-i-N photodiode and electrical filter can be considered as a linear devices.

A. Transmitter

The laser diode is modeled using the spatially averaged model from [4]:

$$\frac{dn}{dt} = \frac{I_b(t)}{Ve} - v_g \frac{G_n(n-n_0)}{1+\varepsilon s} - A_r n - B_r n^2 - C_r n^3, \quad (1)$$

$$\frac{ds}{dt} = \Gamma v_g \frac{G_n(n-n_0)}{1+\varepsilon s} - \frac{s}{\tau_{ph}} + \frac{R}{V}, \quad (2)$$

$$\frac{d\Phi}{dt} = \alpha_L \left[\Gamma v_g G_n (n-n_0) - \frac{1}{\tau_{ph}} \right], \quad (3)$$

where n and s are the average density of carriers and photons, respectively, in the laser active zone, $\Phi(t)$ is the phase of the electric field, $I_b(t)$ is the laser bias current, while e is electron charge. Other laser parameters are described in table I. It should be noted that the equation (3) is given in form like in [2].

The laser parasitics are modeled as a series resistance and parallel capacitance similarly to [1], [4]:

$$\frac{dI_b}{dt} = \frac{I_d - I_b}{\tau_L}, \quad (4)$$

where $I_d(t)$ is the laser driver current and τ_L is the laser parasitics circuit time constant. The output power per one facet $P(t)$ of the laser is given by

$$P(t) = \frac{\eta h \nu V s}{2\Gamma \tau_{ph}}, \quad (5)$$

where ν is the optical frequency, η is differential quantum efficiency and h is the Planck constant.

M. Cvetković is with the Faculty of Technology and Metallurgy, University of Belgrade, P.O.Box 35-03, Karnedžijeva 4, 11120 Belgrade, Yugoslavia

P. Matavulj, J. Radunović and A. Marinčić are with the Faculty of Electrical Engineering, University of Belgrade, P.O.Box 35-54, Bulevar Revolucije 73, 11120 Belgrade, Yugoslavia

E-mail: matavulj@kiklop.etf.bg.ac.yu

0-7803-5235-1/99/$10.00 © 1999 IEEE

B. Optical fiber

We assume that the laser output signal is ideally coupled with optical fiber. Envelope of the input electrical field of the signal injected into the optical fiber is of the form

$$E_{in}(t) = \sqrt{P(t)}e^{j\Phi(t)}. \tag{6}$$

The pulse response of the single-mode optical fiber is given by [2]

$$h_f(t) = \sqrt{\frac{c}{2\lambda^2 DL}}(1-j)e^{-j\frac{\pi c t^2}{\lambda^2 DL}}, \tag{7}$$

where c is the light velocity in vacuum, D is fiber dispersion, L is the fiber length and λ is the optical wavelength.

The output optical power from the fiber is given by [4], [5]

$$P_f(t) = A_f|E_{in}(t) * h_f(t)|^2, \tag{8}$$

where A_f is the fiber attenuation, while operation $*$ denotes convolution.

C. Receiver

In our previous papers, the derivation of the pulse response has been developed for various P-i-N photodiode configurations [6], [7], [8]. The output time domain response of the P-i-N photodiode calculated by the convolution, when the input optical signal has the form of square or sine wave, have been described in [9].

In the equivalent circuit of the photodiode the resistance of the diode contacts and parasitic capacitance of the external circuitry are omitted, while the P-i-N photodiode capacitance is taken into account via the displacement current. During the detection of the incident radiation, the photodiode generates photocurrent which causes a voltage drop on the load resistance, and thus changes the photodiode voltage:

$$U(t) = V_{cc} - U_R(t) = V_{cc} - RI(t). \tag{9}$$

This causes a perturbation of the electric field controlling the carriers transport, inducing in turn photocurrent to change and nonlinearity effects to appear.

In our analysis we consider a InGaAs P-i-N photodiode. The effects of the space charge are omitted. In such case the electric field perturbation in the depletion region is caused only by the change of bias voltage. We assume the semiconductor doping level in the i-region to be low, so that the electric field in this region is homogeneous. We also assume that the length of the i-region is much larger than that of p- and n-regions, therefore the photon absorption in the latter two regions, and hence the diffusion currents, may be neglected. Finally, the reverse bias voltages are assumed not to be very high, and we can assume that mobility of the holes and electrons μ_p and μ_n, respectively, are constant. We also omit recombination and thermal generation in the appropriate continuity equations for electrons and holes.

We assume that the pulse response of the P-i-N photodiode is induced by the power of the incident radiation $P(t)$ given by

$$P_f(t) = W\delta(t), \tag{10}$$

where W is the energy of the incident radiation.

Under all these assumptions and after transforming and solving the set of basic P-i-N photodiode equations, the pulse response of the P-i-N photodiode $h_{ph}(t)$ for $t \geq 0^+$ is given by [7]:

$$h_{ph}(t) = V_{cc} - V_D - V(t), \tag{11}$$

where V_D is the punch-through voltage, and $V(t)$ is given in the implicite form as

$$\begin{aligned} -t &= Y \ln\left|\frac{V(t) - \frac{Z}{X}}{V(0^+) - \frac{Z}{X}}\right| - X \ln\left|\frac{V(t)}{V(0+)}\right| \\ &+ Z\left(\frac{1}{V(t)} - \frac{1}{V(0^+)}\right), \; 0^+ \leq t \leq t_{en}, \end{aligned} \tag{12}$$

$$\begin{aligned} -(t - t_{en}) &= Y_1 \ln\left|\frac{V(t) - \frac{Q}{X_1}}{V(t_{en}) - \frac{Q}{X_1}}\right| - X_1 \ln\left|\frac{V(t)}{V(t_{en})}\right| \\ &+ Q\left(\frac{1}{V(t)} - \frac{1}{V(t_{en})}\right), \; t_{en} \leq t \leq t_{ep}, \end{aligned} \tag{13}$$

$$\begin{aligned} V(t) &= (V_{cc} - V_D) + [V(t_{ep}) - (V_{cc} - V_D)], \\ &t_{ep} \leq t < +\infty. \end{aligned} \tag{14}$$

Symbols τ, Z, Q, X, X_1, Y, and Y_1 from (12)-(14) are given by

$$\tau = \frac{R\varepsilon S}{d}, \; Z = \frac{a_1^2 + a_2^2}{\alpha a_1 a_2 (a_1 - a_2)}, Q = \frac{1}{\alpha a_2},$$

$$X = \frac{C}{V_{cc} - V_D} Z, \; X_1 = \frac{C_1}{V_{cc} - V_D} Q, \; Y = \frac{\tau}{C} + X,$$

$$Y_1 = \frac{\tau}{C_1} + X_1,$$

respectively. In above definitions, ε, S, d and α are explained in table I, while a_1, a_2, C and C_1 are given by

$$a_1 = \frac{\mu_n}{d}, \; a_2 = \frac{\mu_p}{d}, \; C = 1 + Aa_1 - Aa_2 e^{-\alpha d},$$

$$C_1 = 1 - Aa_2 e^{-\alpha d},$$

respectively, and

$$A = \frac{Rq\lambda W}{hcd}.$$

Time boundaries t_{en} and t_{ep} from (12)-(14) denote the time in which all electrons leave the depletion region and the time in which all holes leave depletion region, respectively. The values of t_{en} and t_{ep} are defined by the relations

$$\int_0^{t_{en}} V(t)\,dt = \frac{d}{a_1}, \int_{t_{en}}^{t_{ep}} V(t)\,dt = d\frac{a_1 - a_2}{a_1 a_2}. \quad (15)$$

Finally, the boundary voltage $V(0^+)$ is defined by

$$V(0^+) = \frac{V_{cc} - V_D}{1 + A(a_1 + a_2)(1 - e^{-\alpha d})}, \quad (16)$$

while $V(t_{en})$ and $V(t_{ep})$ are defined by equations (12) and (13), respectively.

The set of equations (11)-(16) implicitly defines the P-i-N photodiode pulse response $h_{ph}(t)$ that can be calculated numerically. It has been shown in [7] that the P-i-N photodiode is a nonlinear device for high values of incident optical energy W. However, if the level of the incident optical energy is small, the P-i-N photodiode can be considered as a linear device. This assumption enables the implementation of the Green function approach for the calculation of the time domain response and, hence, the detected signal $U_R(t)$ is given by

$$U_R(t) = \mathcal{A}(t) * h_{ph}(t) = \int_0^t \mathcal{A}(t')h_{ph}(t - t')\,dt', \quad (17)$$

where $\mathcal{A}(t) = P_f(t)/W$ is the envelope of the incident radiation power. In equation (17), we assume that $\mathcal{A}(t), h_{ph}(t) = 0$ for $t < 0$ and that W is constant.

After photodetection, the signal has to be filtered before the regeneration of the digital signal by sampler/detector unit. Electrical filter is assumed to be a Butterworth 2-nd order filter. The output from the electrical filter is obtained by convolving the load voltage $U_R(t)$ with the pulse response of the Butterworth 2-nd order filter with $0.65/T$ cut-off frequency, where T is the signal bit time.

III. Results of the computer simulation

The described model of the IM/DD lightwave system was used to simulate 10 Gb/s optical system (pulsewidth 100 ps) described in [10] and mathematically modeled in [4]. The laser diode and the optical fiber parameters are taken from [10], while the photodiode parameters are taken from [11].

Since the pulse response of the fiber is not a finite function in a numerical calculation, the Hamming-like window function described in [12] can be used to truncate the fiber pulse response. The fiber pulse response

Table 1. Parameters used in computer simulation.

Laser Parameters	Symbol	Value
Active zone volume	V	$1.53 \cdot 10^{-17}\text{m}^3$
Confinement factor	Γ	0.06
Linewidth enhancement factor	α_L	3
Photon lifetime	τ_{ph}	1.9 ps
Nonradiative recombination	A_R	$10^8\ \frac{1}{\text{s}}$
Radiative recombination	B_R	$1.5 \cdot 10^{-16}\ \frac{\text{m}^3}{\text{s}}$
Auger recombination	C_R	$4.5 \cdot 10^{-41}\ \frac{\text{m}^6}{\text{s}}$
Transparent carrier density	N_0	$1.307 \cdot 10^{24}\frac{1}{\text{m}^3}$
Spontaneous emission rate	R	$10^{12}\ \frac{1}{\text{s}}$
Group velocity	v_g	$8.33 \cdot 10^7\ \frac{\text{m}}{\text{s}}$
Differential gain	G_N	$6.5 \cdot 10^{-20}\ \text{m}^2$
Nonlinear gain coefficient	ε	$4 \cdot 10^{-23}\ \frac{1}{\text{m}^3}$
Differential quantum efficiency	η	0.2
Fiber Parameters	**Symbol**	**Value**
Fiber attenuation	A_f	$0.22\ \frac{\text{db}}{\text{km}}$
Fiber dispersion	D	$16\ \frac{\text{ps}}{\text{nm·km}}$
Photodiode parameters	**Symbol**	**Value**
Absorption coefficient	α	$8 \cdot 10^3\ \text{cm}^{-1}$
P-i-N active area	S	$700\ \mu\text{m}^2$
Width of the i-region	d	2.5, 3, 3.5 μm
Mobility of electrons	μ_n	$1.2\ \frac{\text{m}^2}{\text{Vs}}$
Mobility of holes	μ_p	$0.03\ \frac{\text{m}^2}{\text{Vs}}$
Load resistance	R	10 Ω
Punch-through voltage	V_D	0.6 V
Bias voltage	V_{cc}	3 V
Relative dielectric permitivity	ε_r	13.85

is approximated with $n_f = 500$ samples taken with sampling rate $T_{sf} = 1$ ps.

Photodiode load voltage pulse response $h_{ph}(t)$ is calculated at $n_{ph} = 200$ sampling points with sampling rate $T_{sph} = 1$ ps. These values of parameters are justified if the condition $n_{ph}T_{sph} > t_{ep}$ is fulfilled, since $h_{ph}(t) \approx 0$ for $t \geq t_{ep}$. This condition is fully satisfied for the parameters from Table 1. Although the pulse response $h_{ph}(t)$ can be truncated and smoothed using the various window function, we assume that simple square window function is used, i.e. no special window function is used to correct the approximated pulse response. This is justified with the fact that the significant part of the pulse response $h_{ph}(t)$ is bounded with $0 < t \leq t_{ep}$ [13]. We also take that $W = 1$ fJ which allows us to consider the P-i-N photodiode as a linear device. It can be shown for the given set of parameters that the P-i-N photodiode behaves as a linear device for $W < 10$ fJ.

Driver current amplitude is 20 mA while driver bias current is 50 mA. Rise and fall times of the driver pulses are 50 ps, while the laser parasitics time constant is 15 ps. The input electrical signal, output optical power from fiber that is 50 km long and load voltage from the P-i-N photodiode with i-region width $d = 2.5\,\mu$m are shown in Figure 1. The plot of output optical power from fiber is almost identical to equivalent plot from [4]. The tendency of signal filtering by photodiode can be clearly distinguished. The electrical receiver filtering can be improved with a proper selection of non-material P-i-N photodiode parameters.

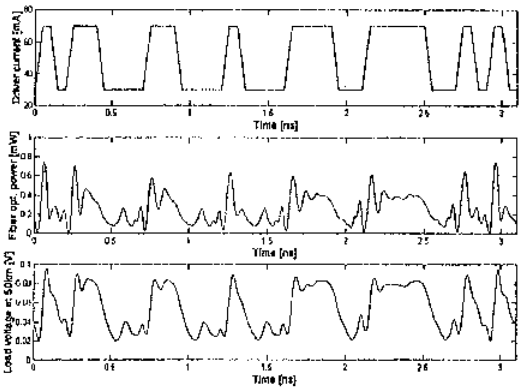

Fig. 1. Input electrical signal, output optical power from fiber and load voltage of the P-i-N photodiode. The optical fiber is 50 km long.

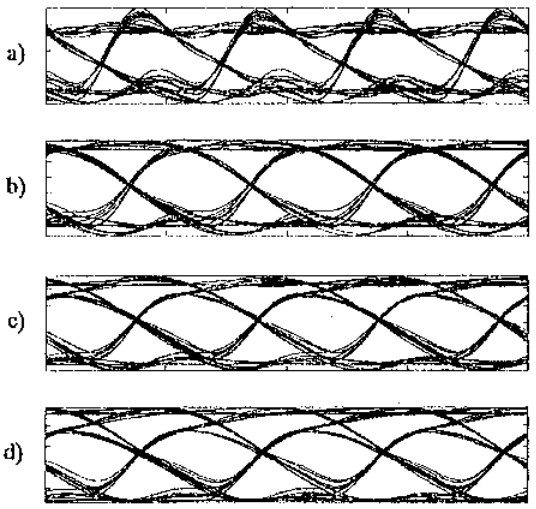

Fig. 2. Eye diagrams of the received signal with ideal square-law detector (a) and P-i-N photodiode with $d = 2.5\,\mu$m (b), $d = 3\,\mu$m (c) and $d = 3.5\,\mu$m (d). Butterworth 2nd order filter with 6.5 GHz cutoff frequency and 50 km long fiber have been employed.

Figure 2 contains the eye-diagram of the output electrical signal from the electrical receiver filter with 6.5 GHz cutoff frequency when optical system operates with ideal square-law photodetector [4] and with P-i-N photodiode with i-region width $d = 2.5\mu$m, $d = 3\mu$m and $d = 3.5\mu$m. The overshoot in eye-diagram is almost completely reduced with $d = 2.5\,\mu$m (Figure 2.(b)) comparing to case with ideal square law photodetector (Figure 2.(a)), and to the case with 4-th order Butterworth filter implementation [4]. However, further increase of d leads to the lower photodiode bandwidth and evident eye-closure (Figure 2.(c) and 2.(d)). We found that the variation in value of cross-section area does not significantly change the response of the photodiode. It should be noted that the stronger filtering does not lead to the noticeable improvement of maximum achievable transmission distance of the lightwave system. Similar behaviour can be observed for different set of parameters.

IV. Conclusion

We have shown that the implementation of the P-i-N photodiode with limited bandwidth in IM/DD optical communication system leads to the reduction of the signal overshoot at the receiver side. The eye-opening of the received and filtered signal can be adjusted by proper selection of i-region thickness of P-i-N photodiode. Described analysis opens a possible way to investigate P-i-N photodiode as a pre-electric filter device which remains as a task for the future work.

References

[1] P. J. Corvini and T. L. Koch, "Computer Simulation of High-Bit-Rate Optical Fiber Transmission Using Single-Frequency Laser", *J. Lightwave Technol.*, Vol. 5, No. 11, November 1987, pp. 1591-1595

[2] J. Cartledge and G. Burley, "The effect of Laser Chirping on Lightwave System Performance", *J. Lightwave Technol.*, Vol. 7, No. 3, March 1989, pp. 568-573

[3] P. Lau and T. Makino, "Effects of Laser Diode Parameters on Power Penalty in 10 Gb/s Optical Fiber Transmission Systems", *J. Lightwave Technol.*, Vol. 15, No. 9, September 1997, pp. 1663-1668

[4] K. Vuorinen, F. Gaffiot and G. Jacquemod, "Modeling Single-Mode Lasers and Standard Single-Mode Fibers Using a Hardware Description Language", *IEEE Photon. Technol. Lett.*, Vol. 9, No. 6, June 1997, pp. 824-826

[5] B. E. A. Saleh and M. I. Irshid, "Coherence and Intersymbol Interference in Digital Fiber Optic Communication Systems", *IEEE J. Quantum Electron.*, Vol. 18, No. 6, June 1982, pp. 944-951

[6] J. Radunović and D. Gvozdić, "Nonstationary and Nonlinear Response of a P-i-N Photodiode Made of a Two-Valley Semiconductor", *IEEE Trans. Electron Devices*, Vol. 40, No. 7, July 1993, pp.1238-1241

[7] P. Matavulj, D. Gvozdić, J. Radunović, J. Elazar, "Nonlinear Pulse Response of P-i-N Photodiode Caused by the Change of the Bias Voltage", Int. J. Infrared & Millimeter Waves, Vol. 17, No. 9, 1996, pp. 1519-1528

[8] P. Matavulj, D. Gvozdić, J. Radunović, "Influence of Nonstationary Carrier Transportion on the Bandwidth of P-i-N Photodiode", *J. Lightwave Technol.*, Vol. 15 No. 12, December 1997, pp. 2270-2277

[9] Lj. Blažević, D. Gvozdić and J. Radunović, "Simulation of the time response of the photodetector", Proc. 2nd Serbian Conf. on Microelectronics and Optoelectronics, MIOPEL'93, Niš, October 26-28, 1993, pp. 225-230

[10] S. Mohrdiek, H. Burkhard, F. Steinhagen, H. Hillmer, R. Lösch, W. Shlapp and R. Göbel, "10-Gb/s Standard Fiber Transmission Using Directly Modulated 1.55-μm Quantum-Well DFB Lasers", *IEEE Photon. Technol. Lett.*, Vol. 7, No. 11, November 1995, pp. 1357-1359

[11] A. F. Sallem and K. F. Brennan, "Theoretical Study of the Response of InGaAs Metal-Semiconductor-Metal Photodetectors", *J. Quantum Electron.*, vol. 31, No. 5, May 1995, pp. 944-953

[12] M. Jackson and G. Burley, "Modeling dispersive fibers with a circuit simulator", *Electron. Lett.*, Vol. 30, No. 15, July 1994, pp. 1245-1246

[13] M. Cvetković, P. Matavulj and A. Marinčić, "Modelling P-i-N Photodiode Time Domain Response Using the Green Function Approach", Proc. TELFOR'98, Belgrade, 24-26.11.1998, pp. 475-478